JOURNAL OF GUIDANCE, CONTROL, AND DYNAMICS
Vol. 29, No. 4, July–August 2006

Trajectories to and from the Lagrange Points and the Primary Body Surfaces

Hexi Baoyin* and Colin R. McInnes†
University of Strathclyde, Glasgow, Scotland G1 1XJ, United Kingdom

This paper investigates ballistic trajectories to and from the vicinity of the Lagrange points L_1 and L_2 and the surfaces of the primaries in the circular restricted three-body problem. The study focuses on trajectories from the Lagrange points and their Lyapunov orbits that can access the entire surfaces of the primary bodies for the sun–Earth and Earth–moon systems. By a symmetry property, trajectories leaving the surface of the primary bodies and reaching the Lagrange points and their Lyapunov orbits can also be found. The lowest velocity increment providing such whole-surface coverage from the Lagrange points and the lowest-energy Lyapunov orbit providing whole-surface coverage are found. Applications of such trajectories are to be found in sample return missions and future crewed missions that use the Lagrange points as exploration staging posts.

Introduction

SINCE 1978, six sun–Earth Lagrange point missions have been flown and others are in development.[1] A systematic study of halo orbit theory was initiated by Farquhar et al,[2,3] and Farquhar and Kamel[4] and after the works of Richardson,[5] Breakwell and Brown,[6] Howell et al.,[7] and Howell,[8] halo orbits around the Lagrange points have been investigated in great detail. The most significant progress in this field has been finding invariant manifolds and the application of nonlinear dynamical systems theory to space mission design. Because of its low fuel consumption and elegant ballistic trajectory, the Genesis mission[7] stimulated great interest in the application of nonlinear dynamical systems theory to design space missions. Canalias et al.,[1] Howell et al.,[7] Howell,[8] Gomez et al.,[9] Koon et al.,[10–13] Lo and Ross,[14] and Ross[15] have made contributions to the field. Lo and Ross presented the concept of the Interplanetary Superhighway and lunar Lagrange point getaway[14] to use connections among the Lagrange points to achieve low-energy transfers from the Earth to the moon or other bodies. Using dynamical system theory Koon et al.[12] provide a comprehensive explanation of the Japanese low-energy lunar mission Hiten, whose trajectory was based on the work of Belbruno and Miller.[16] These studies show that the Lagrange points of the solar system are one of the most important features of multibody dynamics.

Trajectories from the Lagrange points to the primaries of the restricted three-body problem have been investigated previously. Broucke[17] studied trajectories from the Earth–moon Lagrange points to the moon in some detail, and provided a relationship between the initial flight path angle, energy, and flight time. In almost the same way, Prado[18] studied trajectories between the Earth–moon Lagrange points and the Earth. D'Amario and Edelbaum[19] also investigated the minimum transfer between L_2 and the Earth and moon. They focused on the relationship between initial flight angle, impulse, and arrival time, which also gave the minimum impulse at L_2 for moon arrival.

In this paper we investigate ballistic trajectories to and from the Lagrange points L_1 and L_2, and their Lyapunov orbits, directly to the surfaces of the primaries. In particular, we focus on mapping transfers using these trajectories that access the entire surface of the primaries. Such trajectories are of importance for sample return missions and future crewed missions that use the Lagrange points as exploration staging posts. We consider the circular restricted three-body problem and investigate both the sun–Earth and Earth–moon systems. The lowest velocity increment for whole-surface coverage is found for the following five cases: from the Earth–moon L_1 and L_2 points to the lunar surface (close to the surface for terminal powered descent), from the Earth–moon L_1 point to Earth's surface (atmospheric interface for aerobraking), and from the sun–Earth L_1 and L_2 points to the Earth's surface. The relationship between the initial flight path angle, arrival angle, and transfer time is given. For transfers from Lyapunov orbits to the primaries the following six cases are studied; from the sun–Earth L_1 and L_2 Lyapunov orbits to the Earth, from the Earth–moon L_1 and L_2 Lyapunov orbits to the lunar surface, and from an Earth parking orbit to the sun–Earth L_1 and L_2 Lyapunov orbits. Finally, we provide indirect ballistic transfers to the Earth's surface from a sun–Earth L_1 Lyapunov orbit and a direct ballistic lunar sample return scheme. Again, applications of such trajectories are to be found in sample return missions, and future crewed missions which use the Lagrange points as exploration staging posts.

Circular Restricted Three-Body Problem

We consider the problem in the framework of a planar, circular restricted three-body system. This problem assumes that two point-mass primary bodies revolve around their center of mass in circular orbits under the influence of their mutual gravitational attraction. The third body (of infinitesimal mass) moves in the orbit plane of the two primaries under their gravitational influence. The dimensionless equations of motion in a coordinate system rotating with the two primaries are adopted, in which μ is the mass of the smaller primary and $1-\mu$ is the mass of the larger primary.[20] We will consider two three-body systems, the Earth–moon system with $\mu = 0.0122$ and a separation distance of 3.84×10^5 km and the sun–Earth system with $\mu = 304036 \times 10^{-6}$ and a separation distance of 1.5×10^{-8} km. We also assume that the primaries' surfaces are spheres, but for purposes of analysis, the surfaces are defined as having radii of 6500 km for the Earth and 1766 km for the moon. This assumes that a surface intersecting trajectory will either aerobrake at the Earth's atmospheric interface or perform a terminal powered descent at the moon.

In the rotating frame, as shown in Fig. 1, the two primaries are fixed and the equation of the third body's motion can be given as[20]

$$\ddot{x} - 2\dot{y} = \frac{\partial \Omega}{\partial x} \tag{1a}$$

Received 20 May 2005; revision received 23 October 2005; accepted for publication 27 October 2005.

*Assistant Professor, School of Aerospace, Tsinghua University; baoyin@tsinghua.edu.cn. Member AIAA.

†Professor, Department of Mechanical Engineering; colin.mcinnes@strath.ac.uk. Member AIAA.

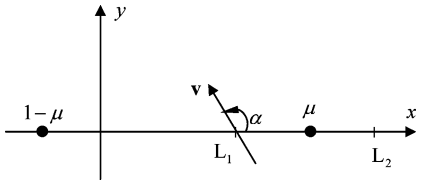

Fig. 1 Definition of the coordinate system and the arrival angle.

$$\ddot{y} + 2\dot{x} = \frac{\partial \Omega}{\partial y} \tag{1b}$$

where

$$\Omega = (x^2 + y^2)/2 + (1-\mu)/r_1 + \mu/r_2 \tag{2a}$$

$$r_1^2 = (x+\mu)^2 + y^2 \tag{2b}$$

$$r_2^2 = (x-1+\mu)^2 + y^2 \tag{2c}$$

Differential equation (1) possesses only one invariant quantity, the well-known Jacobian integral, which can be defined as

$$C = 2\Omega - (\dot{x}^2 + \dot{y}^2) \tag{3}$$

Another important property of Eq. (1) is its five equilibrium points, three collinear points, and two equilateral points. Here we focus only on L_1 and L_2, which have attracted great interest in recent years, because of their potential application for space mission design. We note the following:

Symmetry

Equation (1) has an important symmetric property S such that

$$S : \{x, y, \dot{x}, \dot{y}, t\} \rightarrow \{x, -y, -\dot{x}, \dot{y}, -t\} \tag{4}$$

If we have trajectories from the Lagrange points or their Lyapunov orbits to the primaries, the corresponding reverse trajectories from the primaries to the Lagrange points or their Lyapunov orbits can be found by the symmetry property. For example, if we have a stable manifold of a Lyapunov orbit that goes through a point $P(x, y, \dot{x}, \dot{y})$, we can integrate backward from $P'(x, -y, -\dot{x}, \dot{y})$ to get the unstable manifold, which, in fact, is symmetric to the stable manifold, which can be obtained directly from the symmetric property. Therefore, here we investigate only one set of trajectories, because their reverse trajectories can be easily obtained by the symmetry property.

Lagrange Point Lyapunov Orbits and Invariant Manifolds

Another important dynamical property of Eq. (1) is the family of periodic orbits around the equilibrium points. Among them the periodic orbits associated with L_4 and L_5 are Lyapunov stable for a certain range of the mass ratio, and those associated with L_1–L_3 are unstable for any mass ratio.[20] However, the unstable orbits possess stable and unstable invariant manifolds. The invariant manifold is a multidimensional surface embedded in the whole phase space of the system, and orbits starting on the surface will always remain on that same surface. The invariant manifolds are useful for space mission design, because if the stable manifold of a Lyapunov orbit intersects with an Earth parking orbit, one can directly insert the spacecraft onto the stable manifold to transfer to a Lyapunov orbit. Similarly, if the unstable manifold of a Lyapunov orbit intersects with the surface of a primary, the spacecraft can be transferred onto a ballistic trajectory to the surface of the body (with aerobraking at the Earth, or powered terminal descent at the moon). The collinear points also possess the invariant manifolds. In the two-dimensional case the invariant manifolds associated with a collinear point are a central manifold and two lines: one stable and one unstable. According to the method given in Ref. 9, it can easily be verified that those lines cannot intersect the surfaces of any primary in the sun–Earth or Earth–moon system.

Transfers from L_1 and L_2 to the Surfaces of the Primaries

In this section, using numerical integration, we investigate trajectories from the Lagrange points L_1 and L_2 to the surface of the primaries. We focus on transfers from the Lagrange points that can access the entire surface of the Earth and moon and provide the lowest velocity required for such transfers and the one–one correspondence between the initial flight-path angle, the arrival angle, and the transfer time. Here the initial flight angle is defined as the counterclockwise angle between the velocity vector and the positive x-axis. Similarly, as shown in Fig. 1, the arrival angle is also defined as the counterclockwise angle between the velocity vector and the positive x-axis. But for the curve's continuity, sometimes it may take the value $\alpha - 360$. Transfer time is defined as the time from departure to the primary's surface. Again, by the symmetry property, trajectories leaving the surface of the primary bodies and reaching the Lagrange points can also be found.

We now place the spacecraft at L_1 or L_2 and then systematically vary the magnitude and direction (all possible directions from 0 to 360 deg) of the initial velocity vector. Numerical results show that when the velocity is smaller than a critical value, whatever values the flight-path angle takes, there are no direct transfer trajectories from the Lagrange points which provide whole-surface coverage. Then we fix the velocity at the smallest value and change the initial flight angle in a smaller range to find a more accurate one–one correspondence between the initial flight-path angle and the surface-arrival angle. Numerical results yield the smallest velocity required for whole-surface coverage, as listed in Table 1. If the velocity is smaller than another smaller critical value, the spacecraft cannot directly transfer to any point on the primaries at all, and due to the three-body system's nature all orbits become prograde. This has also been found for a related problem described in Ref. 21. The next section will show that these results are also true for transfers from Lyapunov orbits. However, there may then exist indirect trajectories that reach the surfaces of the primaries after reflecting on the zero-velocity surfaces.

Figure 2a shows the family of trajectories from the Earth–moon L_1 point to the moon providing whole-surface coverage. In this figure and the following, the letter "E" means "Earth" and "M" means "moon." Figure 2b shows the correspondence between the initial flight path angle, the arrival angle, and the transfer time. Figures 3a and 3b are the same curves for trajectories from the sun–Earth L_2 point for whole-Earth-surface coverage. The families of trajectories from the Earth–moon L_2 point to the lunar surface, from the Earth–moon L_1 to the Earth's surface, and from the sun–Earth L_2 point to the Earth's surface were also determined. The results are given in Table 1, but the trajectories are omitted due to similarity to Figs. 2 and 3. In Ref. 19, the minimum transfers from L_2 to the moon are given as 235.6 m/s for 48 h and 144.1 m/s for 77 h. This is the minimum velocity requirement for transfer to a place on the Moon in a certain time, but this velocity cannot transfer to the whole surface of the Moon with any initial flight angle.

Transfers Between Lagrange Point Lyapunov Orbits and the Primaries

In this section we consider ballistic trajectories from Lagrange point Lyapunov orbits to the surfaces of the primaries. The method of calculating a Lyapunov orbit is referenced from Refs. 5 and 8; stable and unstable manifolds can be referenced from Ref. 9. In a manner similar to the trajectories from the Lagrange points to the surfaces of primaries, numerical results show that the transfers from Lagrange-point Lyapunov orbits also have the property that trajectories from low-energy Lyapunov orbits cannot access the entire surface of the primaries. If the energy is reduced further, it cannot even directly transfer to any point on the surfaces of the primaries. Transfer from a Lyapunov orbit to the larger of the primaries in the three-body problem is found to be difficult, and indeed for coverage of the smaller primary, a relatively large Lyapunov orbit is required. We implemented the numerical analysis, detailed in Table 2, for the Earth–moon and

Table 1 Transfer from the Lagrange points to primary surfaces

Transfer	Velocity (m/s)	C	Transfer time (days)	Initial flight path angle (deg)
From Earth–moon L_1 to lunar surface	291.5	3.10715773477815	1.5–2.2	17.47–67.70
From Earth–moon L_2 to lunar surface	293.6	3.08982708074122	1.8–2.7	202.49–251.09
Form Earth–moon L_1 to Earth surface	1135.4	1.95628273477815	2.2–3.7	215.63–263.53
Form sun–Earth L_1 to Earth surface	455.8	3.00066536657090	25–33	36.54–65.53
From sun–Earth L_2 to Earth surface	456.7	3.00066039681623	25–33	217.07–246.26

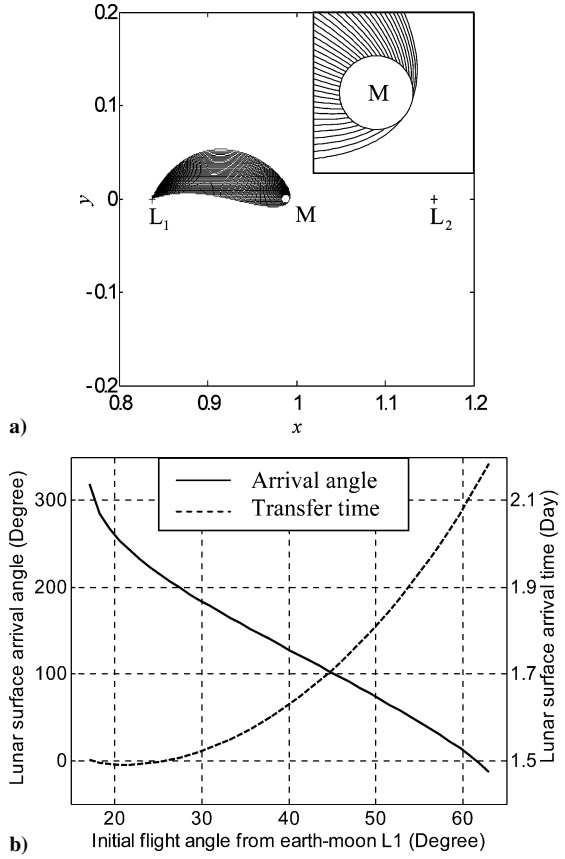

Fig. 2 a) Surface coverage trajectories from the Earth–moon L_1 point to the lunar surface; b) correspondence between initial flight path angle, arrival angle, and transfer time.

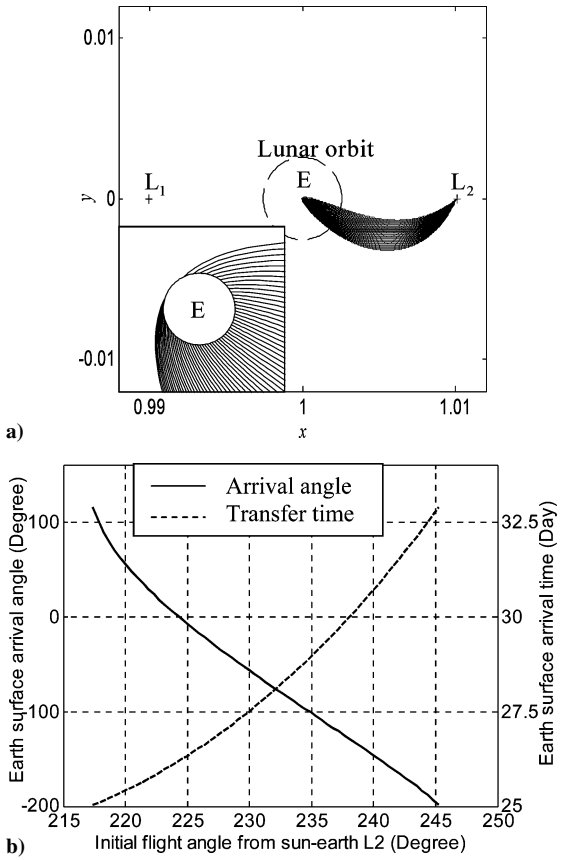

Fig. 3 a) Surface coverage trajectories from the sun–Earth L_2 point to the Earth's surface; b) correspondence between initial flight path angle, arrival angle, and transfer time.

sun–Earth systems. It is found that in the Earth–moon case the smallest Lyapunov orbit that can directly cover the entire surface of the moon has $C = 3.12185282430647$ for an L_1 Lyapunov orbit and $C = 3.09762627497867$ for an L_2 Lyapunov orbit. In the sun–Earth case it is found that $C = 3.00070183603177$ for an L_1 Lyapunov orbit and $C = 3.00070031306437$ for an L_2 Lyapunov orbit. Figure 4a shows a family of direct, whole-Earth surface-coverage trajectories from the sun–Earth L_1 Lyapunov orbit to the Earth's surface (atmospheric interface). Here the amplitude of the y-direction is 0.007676, about 1,151,400 km in dimensional real size. We also investigated other types of whole-surface-coverage transfers from Lyapunov orbits and transfers from Earth parking orbits to sun–Earth Lyapunov orbits, as shown in Table 2. Here we applied a small velocity increment as the initial perturbation to the spacecraft to leave the Lyapunov orbit and enter the stable or unstable manifold. In these cases a small perturbation velocity increment, 1m/s, was applied along the x-direction. The stable manifold is obtained by forward integration and the unstable manifold is obtained by backward integration. In Fig. 4a the star marks indicate the position where the initial perturbations are applied, and Fig. 4b shows the transfer time and arrival angle. Note that here the transfer time depends on the magnitude and position of the initial perturbation. Comparing the Jacobian constants in Tables 1 and 2, it can be seen that whole-surface coverage from Lyapunov orbits requires a lower energy than that from Lagrange points, but the transfer time is longer.

The design procedure for transfers from Earth parking orbits to a Lyapunov orbit is usually based on a shooting method. However, the stable manifold offers an alternative method. For a Lyapunov orbit with energy smaller than a critical value there is no direct transfer from an Earth parking orbit to the Lyapunov orbit, because they do not intersect each other. Here we numerically obtain the smallest Lyapunov orbit whose stable manifold intersects with an Earth parking orbit for the sun–Earth system. The results are listed in the last two rows of Table 2. The altitude of the Earth parking orbit is taken as 222 km, and lunar perturbations are not considered. Figure 5 shows the stable manifolds of the smallest sun–Earth Lyapunov orbits that intersect with the Earth parking orbit defined above. But the stable or unstable manifolds of a normal Earth–moon L_1 or L_2 Lyapunov orbit do not intersect with an Earth parking orbit.

Indirect Ballistic Transfers and Connected Periodic Orbits

As noted earlier, if a Lyapunov orbit is too small, then direct ballistic trajectories providing whole-surface coverage, or even transfers to any location on the surface of a primary, do not exist.

Table 2 Jacobian constant and transfer time from smallest Lyapunov orbits

Transfer	C	Transfer time (days)
From Earth–moon L_1 halo to lunar surface	3.12185282430647	∼11
From Earth–moon L_2 halo to lunar surface	3.09762627497867	∼14
Form sun–Earth L_1 halo to Earth surface	3.00070183603177	∼172
From sun–Earth L_2 halo to Earth surface	3.00070031306437	∼175
Form Earth parking orbit to sun–Earth L_1 halo	3.00081946031763	∼165
From Earth parking orbit to sun–Earth L_2 halo	3.00081513373089	∼167

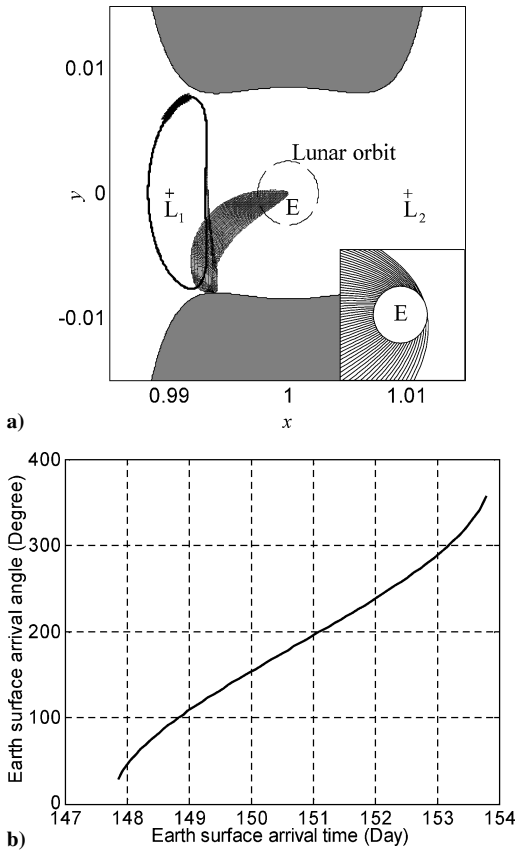

Fig. 4 a) Surface coverage trajectories from sun–Earth L_1 Lyapunov orbit to the Earth's surface; b) arrival time and arrival angle from sun–Earth L_1 Lyapunov orbit to the Earth's surface.

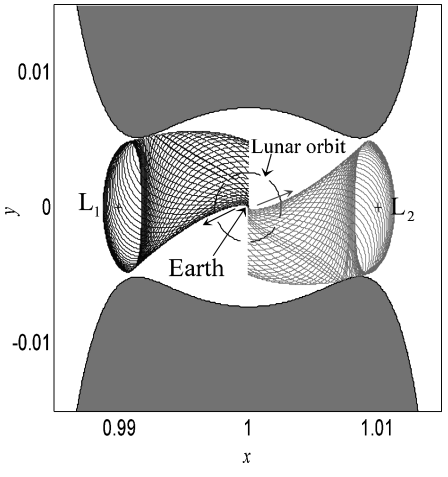

Fig. 5 Stable manifolds of the smallest Lyapunov orbit that intersects the Earth parking orbit.

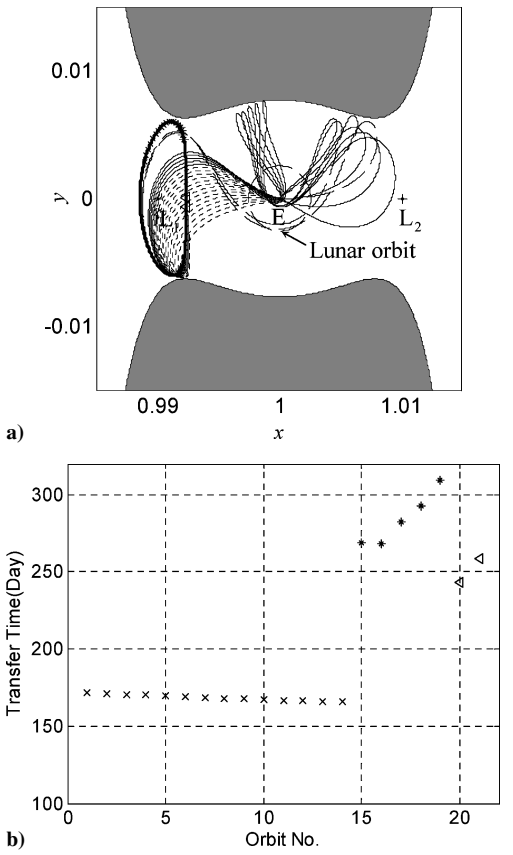

Fig. 6 a) Direct and indirect transfers from the sun–Earth L_1 Lyapunov orbit to the Earth's surface; b) transfer time for trajectories shown in Fig. 5a.

However, some indirect trajectories may exist, similar to the indirect ballistic transfer from a sun–Earth Lyapunov orbit to Earth's surface (atmospheric interface) of the Genesis mission. In the previous two sections we have discussed direct transfer to the surface of the primaries, but for indirect transfer there is a different-energy Lyapunov orbit with a particular unstable manifold. Some Lyapunov orbits have a manifold of only prograde unstable orbits, while some have prograde and retrograde orbits simultaneously. We have found several families of indirect transfers numerically. Figure 6a shows some direct transfers (dotted line) and two types of indirect transfers from a sun–Earth L_1 Lyapunov orbit to the Earth's surface, with $C = 3.00077466890398$. Again, the marks " $\times$ " "$*$," and "$\triangleleft$" indicate the locations where the initial perturbations are applied. Among them the dashed line trajectories, which are similar to the Genesis mission, are reaching the Earth's surface after only one reflection on the zero-velocity curve. The solid-line trajectories are a different family of indirect transfers that reach the Earth's surface after two reflections on the zero-velocity curve. Figure 6b shows the transfer time of these 21 trajectories, the marks corresponding to Fig. 6a. Indirect transfers required approximately 3 months longer than direct transfers. However, the transfer type and transfer time again depend on the initial perturbation, with a larger perturbation shortening the transfer time and possibly changing the transfer type.

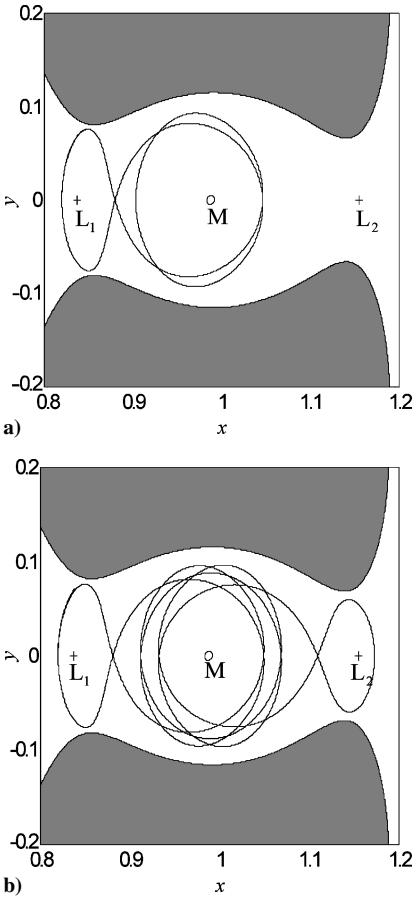

Fig. 7 a) Double lunar homoclinic periodic orbit; b) double lunar heteroclinic periodic orbit.

If the energy of a Lyapunov orbit increases further, the Genesis-like indirect transfers can disappear, and the trajectory becomes much more complicated. Among the more complicated trajectories found are several families of periodic orbits that are associated with the Lyapunov orbits. Figure 7 shows two families of double periodic orbits in the Earth–moon system, similar to the single homoclinic and heteroclinic orbits that have been found in Ref. 10. These numerical results show that in fact homoclinic or hetoroclinic orbits with multiple periodicity can also be found.

Ballistic Lunar Sample Return

There is growing interest in a return to the moon using both robotic surface landers and crewed missions. Using the concept of the Interplanetary Superhighway, Ref. 22 provides several types of low-energy lunar-sample return schemes. Here we investigate another type of low-energy lunar-sample return, using direct ballistic transfers between the Earth and moon. From the trajectories between the Lagrange points and the primaries, it is clear that low-energy ballistic transfers between the Earth and moon cannot be found in the vicinity of L_1. However, to determine a direct ballistic transfer from the moon to the Earth, we can use the unstable manifold of a sun–Earth Lyapunov orbit.

First, we determine the unstable manifold of a sun–Earth Lyapunov orbit and transform it into the Earth–moon rotating coordinate system. We then find a trajectory that traverses the vicinity of the moon, which we regard as a reference trajectory. Figure 8a shows some unstable manifold (dotted lines of Fig. 6a) trajectories transformed into Earth–moon rotating coordinates. Among these trajectories the solid line trajectory is passing through the lunar surface, and so can be used as a reference trajectory to generate a moon-to-Earth direct ballistic transfer. Finally, between the Earth and moon we take a point on this trajectory, from which we integrate forward and backward to obtain a trajectory from the lunar surface

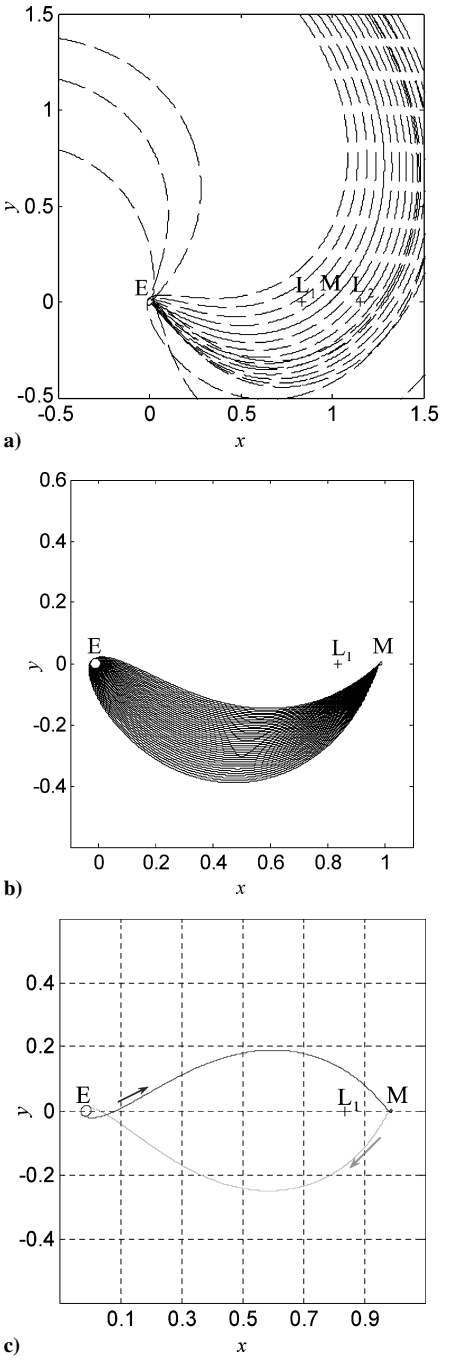

Fig. 8 a) Sun–Earth halo orbit unstable manifold plotted in Earth–moon frame; b) ballistic trajectories from the lunar surface to the Earth's surface using the unstable manifold of a sun–Earth halo orbit; c) lunar sample return trajectory generated using the unstable manifold of a sun–Earth Lyapunov orbit.

to the Earth in the Earth–moon system. The difference between the trajectory obtained and the reference trajectory is due to solar perturbations, because in the Earth–moon system solar perturbations are not considered. The results, however, show that in this case the difference is very small. Varying the initial states on the lunar surface, one can obtain a set of trajectories that map onto the Earth's surface. Figure 8b shows trajectories from a single point on the lunar surface to the Earth's surface (atmospheric interface for aerobraking). We can then find similar trajectories from other points on the lunar surface, with the takeoff velocity requirement for a ballistic transfer of order 2500–2800 m/s. Figure 8c shows a complete lunar sample return scheme generated by this method, where the spacecraft is injected from a 200-km Earth parking orbit and lands on the Earth side of the lunar surface. For illustration, the

Table 3 Lunar sample return trajectory requirements

	Duration (days)	Δv (m/s)
Injection from Earth	——	3090
Lunar landing	3.03	2558
Lunar take-off	——	2558
Earth return	3.35	——
Total	6.38	8196
Conic section method	9.08	9506[a]

[a]Reference 22.

vehicle takes off from the same location on a direct ballistic return to the Earth. The total trip time is less than 1 wk, and the energy need is low, being approximately 14% less than from the conventional conic section method, as detailed in Table 3.

Conclusions

This paper investigated ballistic trajectories from the vicinity of the Lagrange points L_1 and L_2 to the surfaces of the primaries in the circular restricted three-body problem. In particular, the study focused on the trajectories from the Lagrange points and their Lyapunov orbit, which provided whole-surface coverage for the sun–Earth and Earth–moon systems. The lowest velocity increment that provided whole surface coverage was found for trajectories from the Earth–moon L_1 and L_2 points to the moon, from the Earth–moon L_1 point to the Earth, and from the sun-Earth L_1 and L_2 points to the Earth. Because of the particular flow near the Lagrange points, if the velocity increment is smaller than some critical value, whatever values the initial flight path angle takes, there are no trajectories which provide whole surface coverage. The relationship between the initial flight path angle, arrival angle and transfer time is provided. Applications of such trajectories are to be found in sample return missions, and future crewed missions which use the Lagrange points as exploration staging posts.

For transfers from Lyapunov orbits to the primaries, trajectories from the sun–Earth L_1 and L_2 Lyapunov orbits to the Earth, from the Earth–moon L_1 and L_2 Lyapunov orbits to the lunar surface, and from an Earth parking orbit to the sun–Earth L_1 and L_2 Lyapunov orbits were investigated. Because of the Lyapunov orbit invariant manifold structure, small Lyapunov orbits do not provide direct ballistic transfers providing whole-surface coverage of the primaries. Indeed, if the Lyapunov orbits become small enough, they do not have a direct transfer to any location on the primaries. Finally, a low-energy, ballistic lunar sample return trajectory is provided, which requires a velocity increment of order 14% less than the conventional patched conic method.

References

[1]Canalias, E., Gomez, G., Marcote, M., and Masdemont, J. J., "Assessment of Mission Design Including Utilization of Libration Points and Weak Stability Boundaries," *ESA Advanced Concept Team*, URL: http://www.esa.int/act [cited 14 Jan. 2005].

[2]Farquhar, R. W., Muhonen, D. P., and Richardson, D. L., "Mission Design for a Halo Orbiter of the Earth," *Journal of Spacecraft and Rockets*, Vol. 14, No. 3, 1977, pp. 170–177.

[3]Farquhar, R. W., Muhonen, D. P., Newman, C. R., and Heuberber, H. S., "Trajectories and Orbital Maneuvers for the First Libration-Point Satellite," *Journal of Guidance and Control*, Vol. 3, No. 6, 1980, pp. 549–554.

[4]Farquhar, R. W., and Kamel, A. A, "Quasi-Periodic Orbits About the Translunar Libration Point," *Celestial Mechanics*, Vol. 7, June 1973, pp. 458–473.

[5]Richardson, D. L., "Analytic Construction of Periodic Orbits About the Collinear Points," *Celestial Mechanics*, Vol. 22, Oct. 1980, pp. 241–253.

[6]Breakwell, J. V., and Brown, J. V., "The 'Halo' Family of 3-Dimensional Periodic Orbits in the Earth–Moon Restricted 3-Body Problem," *Celestial Mechanics*, Vol. 20, Nov. 1979, pp. 389–404.

[7]Howell, K. C., Barden, B., and Lo, M., "Application of Dynamical Systems Theory to Trajectory Design for a Libration Point Mission," *Journal of the Astronautical Sciences*, Vol. 45, No. 2, 1997, pp. 161–178.

[8]Howell, K. C., "Three-Dimensional, Periodic, 'Halo' Orbit," *Celestial Mechanics*, Vol. 32, No. 1, 1984, pp. 53–71.

[9]Gomez, G., Jorba, A., Masdemont, J., and Simo, C., "Study of the Transfer from the Earth to a Halo Orbit Around the Equilibrum Point L_1," *Celestial Mechanics and Dynamical Astronomy*, Vol. 56, No. 4, 1993, pp. 541–562.

[10]Koon, W. S., Lo, M. W., Marsden, J. E., and Ross, S. D., "Heteroclinic Connections Between Periodic Orbits and Resonance Transitions in Celestial Mechanics," *Chaos*, Vol. 10, No. 2, 2000, pp. 427–469.

[11]Koon, W. S., Lo, M. W., Marsden, J. E., and Ross, S. D., "Resonance and Capture of Jupiter Comets," *Celestial Mechanics and Dynamical Astronomy*, Vol. 81, 2001, pp. 27–38.

[12]Koon, W. S., Lo, M. W., Marsden, J. E., and Ross, S. D., "Low Energy Transfer to the Moon," *Celestial Mechanics and Dynamical Astronomy*, Vol. 81, 2001, pp. 63–73.

[13]Koon,W. S., Lo, M. W., Marsden, J. E., and Ross, S. D., "Constructing a Low Energy Transfer Between Jovian Moons Contemp," *Contemporary Mathematics*, Vol. 292, 2002, pp. 129–145.

[14]Lo, M., and Ross, S., "Low Energy Interplanetary Transfers Using Invariant Manifolds of L_1, L_2 and Halo Orbits," *AAS/AIAA Space Flight Mechanics Meeting*, AAS Paper 98-136, Feb. 1998.

[15]Ross, S., "Statistical Theory of Interior–Exterior Transition and Collision Probabilities," *Libration Point Orbits and Applications*, edited by G. Gomez, M. W. Lo, and J. J. Masdemont, World Scientific, River Edge, NJ, 2003, pp. 637–652.

[16]Belbruno, E., and Miller, J., "Sun-Perturbed Earth-to-Moon Transfers with Ballistic Capture," *Journal of Guidance, Control, and Dynamics*, Vol. 16, No. 4, 1993, pp. 770–775.

[17]Broucke, R., "Travelling Between the Lagrange Points and the Moon," *Journal of Guidance and Control*, Vol. 2, No. 4, 1979, pp. 257–263.

[18]Prado, A. F. B. A., "Travelling Between the Lagrange Points and the Earth," *Acta Astronautica*, Vol. 39, No. 7, 1996, pp. 483–486.

[19]D'Amario, L. A., and Edelbaum, T. N., "Minimum Impulse Three-Body Trajectories," *AIAA Journal*, Vol. 12, No. 4, 1974, pp. 455–462.

[20]Szebehely, V., *Theory of Orbits: The Restricted Problem of Three Bodies*, Academic Press, New York, 1967.

[21]Astakhov, S. A., Burbanks, A. D., Wiggins, S., and Farrelly, D., "Chaos-Assisted Capture of Irregular Moons," *Nature*, Vol. 423, 15 May 2003, pp. 264–267.

[22]Lo, W. M., and Chung, M. J., "Lunar Sample via the Interplanetary Superhighway," URL: http://www.gg.caltech.edu/~mwl/publications/publications2.htm [cited 18 May 2005].